

## STRUCTURE OF HIGH-CARBON STEEL AFTER WELDING WITH RAPID COOLING

Yurii Kalinin<sup>1)</sup>, Michail Brykov<sup>2\*)</sup>, Ivan Petryshynets<sup>3)</sup>, Vasily Efremenko<sup>4)</sup>, Olaf Hesse<sup>5)</sup>, Maik Kunert<sup>5)</sup>, Michail Andrushchenko<sup>2)</sup>, Michail Osipov<sup>2)</sup>, Stanislav Berezhnnyy<sup>2)</sup>, Oleg Bykovskiy<sup>2)</sup>

<sup>1)</sup> PJSC Zaporozhtransformator, Zaporizhzhia, Ukraine

<sup>2)</sup> Zaporizhzhia National Technical University, Zaporizhzhia, Ukraine

<sup>3)</sup> Institute of Materials Research Slovak Academy of Sciences, Košice, Slovakia

<sup>4)</sup> Pryazovskyi State Technical University, Mariupol, Ukraine

<sup>5)</sup> Ernst-Abbe-Hochschule Jena, Jena, Germany

Received: 14.05.2019

Accepted: 16.06.2019

\* Corresponding author: [brykov@zntu.edu.ua](mailto:brykov@zntu.edu.ua), Tel: +38 061 7698262, Welding Department, Zaporizhzhia National Technical University, Zhukovsky 64, 69063 Zaporizhzhia, Ukraine

### Abstract

In this paper the effect of rapid cooling during arc welding on the structure of fusion layer and heat affected zone (HAZ) of high-carbon low alloyed steel have been studied. The main idea was that despite of high carbon content (1.2%) it is necessary to achieve quenching in HAZ. Due to proper chemical composition of welded steel martensite start temperature  $M_s$  is about 20 °C, therefore austenitic structure of quenched metal is preserved after rapid cooling. Exposition of HAZ to excessive heat during welding cycle leads to local precipitation of carbides from austenite and thus raising of  $M_s$ . In this case some amount of martensite was present in structure after cooling along with austenite and carbides. Microstructure, microhardness and chemical composition of remelted electrode metal, fusion zone and HAZ were studied by means of optical microscopy, SEM, EDX and microhardness testing.

**Keywords:** wear resistance, high-carbon low-alloyed steels, welding, rapid cooling, austenite, martensite

### 1 Introduction

Wear is addressed to as one of major problems in modern industry. Any machine part that works in moving contact under load with some counter body always suffer from wear, which is gradual loss of material from contact surface. Ultimate wear may vary from several tenths of micrometers, for example in elements of diesel engine fuel pumps [1] or dies for assembling car body parts [2-4] to tenth of millimeters for parts of blast furnaces [5] or milling and crushing equipment in mineral processing industries working under abrasive wear [6].

Reducing wear loss may be achieved in several ways. Widely used methods are deposition of protective layers by surfacing [7-9], optimization of bulk heat treatment [10, 11, 12] or surface modifying treatment [13-16] of properly chosen wear resistant compositions. Recently new class of wear resistant materials for abrasive wear environment is proposed. That is high-carbon low-alloyed steels [17-19]. Due to high carbon concentration (1.2%) and about 3% of alloying elements it is possible to reduce martensite start temperature  $M_s$  as low as to 10-30 °C when quenching from single-phase  $\gamma$ -domain. Therefore the amount of retained austenite after quenching these steels in water at room temperature achieves 90-100% [19]. Because of high

sensitivity of that austenite to phase transformation under mechanical impact – for example scratching during abrasive wear – thin hard layer (up to 11 GPa depending on abrasive conditions) of mechanically induced martensite is instantly forming on worn surface enabling higher abrasive wear resistance of steel [19].

High carbon content is beneficial for wear resistance of steel but simultaneously worsens its weldability. Steels with carbon equivalent 0.4 and higher are considered to have poor weldability [20, 21]. It is well-adopted that the higher carbon or other alloying elements (except Co) are present in austenite the less is a cooling rate needed to avoid formation of martensitic structure [22]. Therefore the more carbon and other elements are contained in steel (carbon equivalent) the more probable is appearing of martensite in heat affected zone (HAZ) after welding which leads to cracks in HAZ (i.e. steel poor weldability). Preheating these steels before welding leads to decreasing cooling rate in HAZ below critical level hence martensite formation can be suppressed. Post-welding heat treatment provides decomposition of martensite if any appears within HAZ during welding thermal cycle.

Steels with carbon content above 0.5-0.8 wt.% are not widely used in welding joints. Ms temperature for carbon concentrations 0.5-0.8 wt.% is high enough, therefore the retained austenite in HAZ is not considered as a factor influencing mechanical properties. If for some reasons Ms is decreased to room temperature or lower, then martensite would not be present in HAZ at all, and all efforts aimed to avoid martensite formation (pre-heating and post-welding heat treatment) would not be necessary. This is the case for welding high-carbon (about 1.2 wt.%) low-alloyed (about 3 wt.% of alloying elements in total) steels which possess 100 vol.% of retained austenite after quenching due to Ms to be at about of 20 °C. Regarding these steels preheating and post-welding thermal treatment would negatively affect the structure of retained unstable austenite, thus abrasive wear resistance of welded parts would be dramatically decreased. Therefore rapid cooling in HAZ is vitally needed to provide fully austenitic structure avoiding pearlite formation in the vicinity of fusion line. This will allow obtaining welding joints with higher wear resistance.

Currently rapid cooling is used at most as technique to improve mechanical properties of HAZ formed during friction stir welding of Al-based alloys [23, 24], Fe-based alloys with different carbon content [25, 26, 27]. Some techniques like explosion welding or laser welding involve rapid cooling without any special efforts [28, 29], although even during laser welding especially accelerated cooling is sometimes necessary [30]. Concluding, rapid cooling is a known technique used in welding however intended rapid cooling in HAZ during welding of high-carbon low-alloyed steels is not studied and substantiated yet.

Basing on above considerations, the object of present work was studying the model weld joint of high-carbon low-alloyed steel focusing on microstructure formed in HAZ under rapid cooling.

## 2 Experimental materials and methods

Industrially manufactured 5mm thick and 60 mm wide strip of steel 120Mn3Si2 was used for welding experiment. Chemical composition of steel was as follows: 1.21 wt% C, 2.56 wt% Mn, 1.59 wt % Si. Rectangular workpiece of this strip was quenched from 1000 °C into water to obtain fully austenitic structure.

Welding with rapid cooling was imitated by fast single touch of electrode with the edge of workpiece. The touch initiated arc spark with current of 130 A at a voltage of 25 V. The reverse polarity was used to increase heat input. As a result single welding “joint” shown in **Fig.1** was formed from base material and remelted electrode metal. The heat generated by the arc was

quickly dissipated through heat conductivity into workpiece. The temperature of HAZ was controlled by chromel-copel thermocouple that was welded to the flat side of workpiece in a distance of 5 mm from its edge. The “Time-Temperature” correlation corresponding to welding cycle is presented in **Fig. 2**.

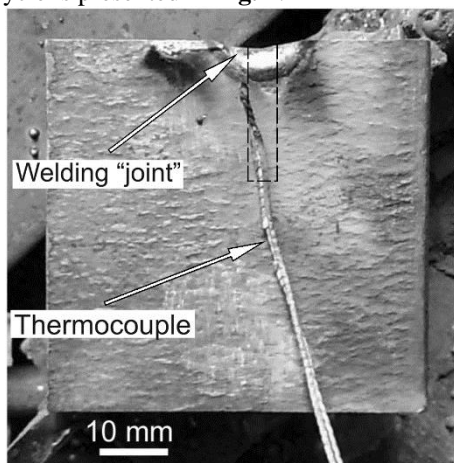


**Fig. 1** Experimental workpiece with single welding “spot”

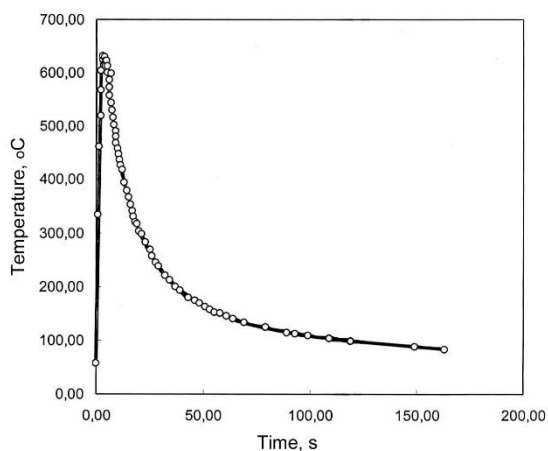


**Fig. 2** “Time-Temperature” correlation corresponding to welding cycle

According to **Fig. 2** thermocouple junction have been almost contacted with liquid metal. Nevertheless the peak temperature was much lower than melting point of steel and even  $A_{c1}$ . This may be explained by very short welding cycle (less than 1 s) and fast cooling due to heat conductivity into cold base metal. As a result, the heat input to thermocouple junction appeared to be insufficient to increase temperature to higher values than that recorded.

The sample of about 20 mm long and about 5 mm wide was cut from the workpiece as shown in **Fig. 1** by dashed line. Sample’s cross-section was polished and etched with 4 vol% nital. Microstructure of HAZ was investigated by means of SEM (JEOL JSM-7000F) and optical microscopy (OLYMPUS GX-71). Local EDX analysis was performed using SEM (TESCAN) equipped with Bruker EDX detector. Microhardness was measured by computer controlled Wilson® Hardness tester.

### 3 Results and discussion

Panorama compiled by low magnification optical micrographs depicting microstructure of welding “joint” and HAZ is shown on **Fig. 3**. Four distinctive structural areas are revealed namely: (a) zone A of light contrast showing remelted electrode material, (b) zone B of uniformly gray contrast, (c) zone C with heterogeneous structure comprising the areas with grey contrast and dark contrast and (d) zone D located from both sides to the depth of about 1.3 mm having mostly dark contrast (the latter was presumably resulted from decarburization during the manufacturing of steel strip).

Results of microhardness measurement of HAZ (C, B) through fusion layer from indent 1 (zone C) to indent 2 (zone A) are shown on **Fig. 4**.

As seen from the **Fig. 4**, the microhardness of indent 1 is 320 HV, then it varies in the range of 240-260 HV in zone B and 240-270 HV in zone A. Sharp increase in microhardness up to 450 HV is noted for narrow layer located between zone B and zone A.

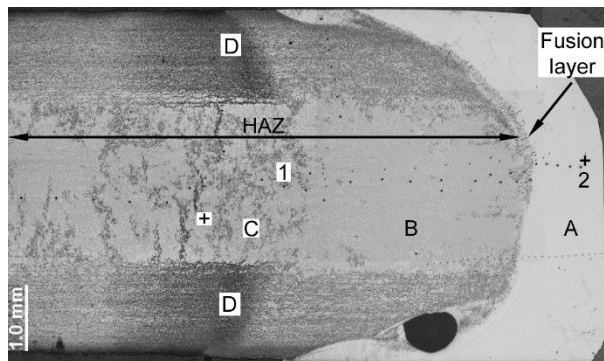


**Fig. 3** Panorama of microstructure of HAZ, fusion layer and remelted electrode metal

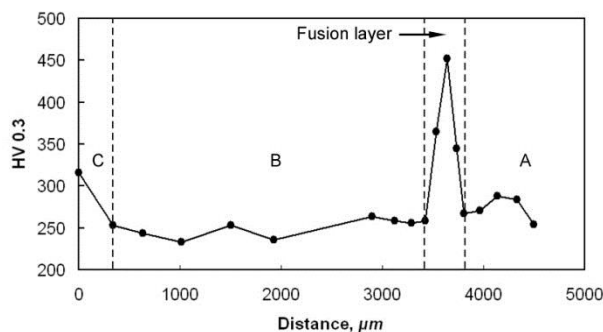


**Fig. 4** Results of microhardness measurement of HAZ, fusion layer and remelted electrode metal

The higher microhardness (320 HV) corresponding to indent 1 in zone C is explained by the presence of heterogeneous structure composed of retained austenite, needle martensite and some portion of nodular carbides (shown as “1” in **Fig. 5, a**). According to microhardness value retained austenite is presumably major phase in the structure of zone C while carbides appeared in HAZ due to austenite decomposition under heat input. In contrast of zone C, the microstructure of zones B (**Fig. 5, b**) and A (**Fig. 5, c**) is fully austenitic which is in accordance with its lower microhardness. However, in fusion layer between zones A and B the needle martensite is revealed again (**Fig. 5, d**) resulting in sharp microhardness increase.

As follows from microstructure observation (see **Fig. 3**), martensite presents in significant amount in zone C and it is almost absent in zone B. Therefore the question arises why martensite presenting in zone C suddenly disappears in zone B making clearly visible “border” between these areas?

The most obvious reason is supposed to be connected with temperature distribution in workpiece under welding heat input. If we assume the exponential mode of temperature distribution in zone B like that on the workpiece surface (see **Fig. 2**) then in zone B temperature rose to higher values than in zone C, to be above  $A_{c_m}$  temperature. Very fast heating suppressed the precipitation of carbides from retained austenite thus retained austenite reached high temperature domain (above  $A_{c_m}$ , **Fig. 6**) without depletion in carbon.

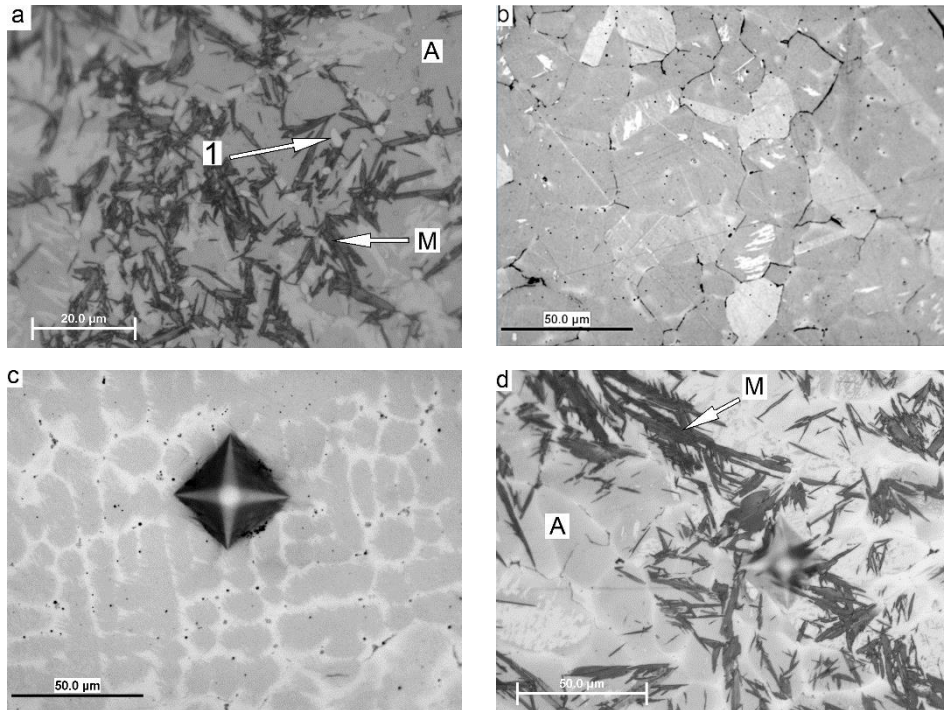


**Fig. 5** Microstructure of different zones: (a) zone C; (b) zone B in the vicinity of fusion layer; (c) zone A near penultimate hardness imprint and (d) fusion layer. (Martensite (M), austenite (A) and carbides (1))

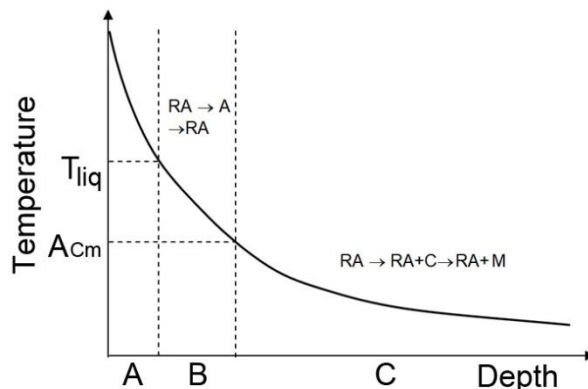


**Fig. 6** Schematic temperature distribution in workpiece from model welding joint inward and corresponded structural zones A, B and C (designations RA, C, M are retained austenite, carbide, martensite accordingly)

Under consequent fast cooling this austenite fully retained in the structure forming zone B. In zone C the temperature was below  $A_{Cm}$  to be enough for carbide precipitation from retained austenite. This process resulted in  $M_s$  point rising which leads to partial transformation of austenite into martensite in zone C during subsequent cooling.

This assumption is revealed by the difference in volume fraction of carbide phase between zones C and B shown in **Fig. 7**. **Fig.7a** depicts the carbides as nodular inclusions and as network along grain boundaries which is characteristic for zone C. In contrast, in **Fig. 7b** carbide network is not detected while nodular carbides are present; this case corresponds to the boundary between zone C and zone B. That means that less carbides precipitated from austenite under weld cycle when moving from zone C to weld.

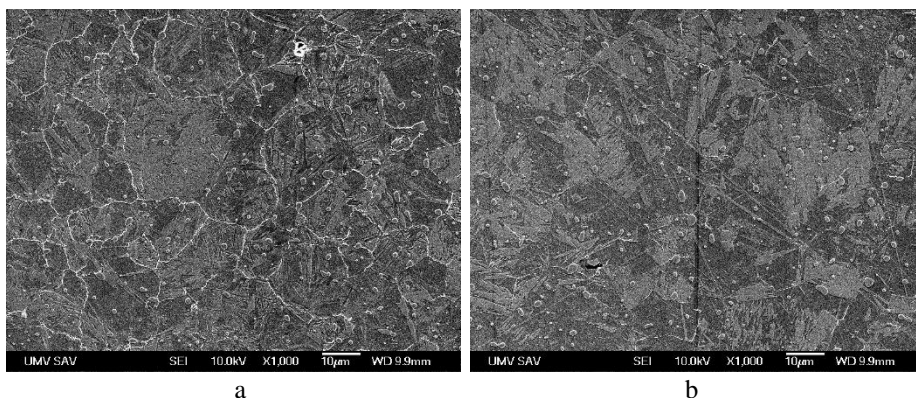


**Fig. 7** Microstructure of transition area from zone C to B: (a) near indent 1 (see **Fig. 3**); (b) on the boundary between zone C and zone B

Panorama of transition from zone B to A through the fusion layer is shown on **Fig. 8**. The magnification is the same as of **Fig. 7**. There are no excessive carbides visible in structure. This proves the assumptions concerning heat influence on structure of HAZ that is expressed above. Appearance of martensite in structure of fusion layer (see **Fig. 5, d**) may be explained by the same considerations as for HAZ. The main reason is local rising of  $M_s$  due to decarburizing (“dilution”) of base metal in fusion layer under melting of electrode material. Excessive alloying of electrode metal by Mn, Cr, Ni may compensate carbon loss and prevent appearance of martensite in fusion layer however this would significantly increase electrodes production costs. Therefore chemical composition of electrode metal should minimally differ from base metal.

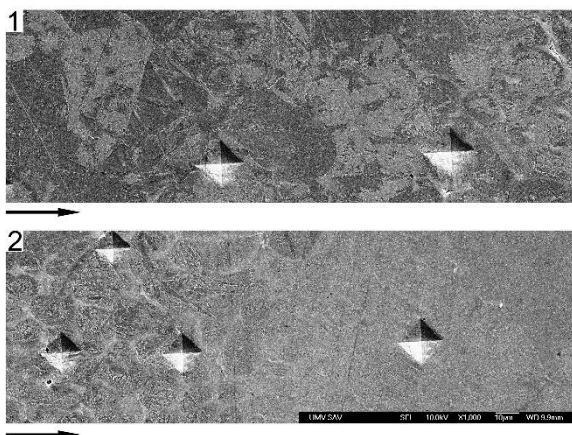


**Fig. 8** Microstructure of transition area from zone B to A

Results of point EDX analyses of base metal and electrode remelted metal are shown on **Fig. 9**. Points of analyses are shown on **Fig. 3** as crosses. According to EDX both base and electrode metals contains approximately equal amount of manganese and silicon, but electrode metal contains 1.5% less of carbon and about 2% of chrome. Detected high values for carbon content should not be taken into account as it is an artifact connected with carbon contamination, which is known weak feature of EDS method. The result of EDX analyses through fusion layer is shown on **Fig. 10**. It is seen that concentration of manganese is approximately the same for base and electrode metal while concentration of chrome rises significantly from base to electrode metal. This result corresponds to that shown on **Fig. 9**.

| Spectrum: Spectrum         |    |          |               |                | Spectrum: Spectrum |                        |                            |    |          |               |                |                |                        |
|----------------------------|----|----------|---------------|----------------|--------------------|------------------------|----------------------------|----|----------|---------------|----------------|----------------|------------------------|
| El                         | AN | Series   | unn. C [wt.%] | norm. C [wt.%] | Atom. C [at.%]     | Error (1 Sigma) [wt.%] | El                         | AN | Series   | unn. C [wt.%] | norm. C [wt.%] | Atom. C [at.%] | Error (1 Sigma) [wt.%] |
| C                          | 6  | K-series | 7,65          | 7,96           | 28,36              | 1,58                   | C                          | 6  | K-series | 6,26          | 6,55           | 24,31          | 1,41                   |
| Si                         | 14 | K-series | 1,35          | 1,40           | 2,13               | 0,10                   | Si                         | 14 | K-series | 1,11          | 1,16           | 1,84           | 0,09                   |
| Mn                         | 25 | K-series | 2,24          | 2,33           | 1,81               | 0,13                   | Cr                         | 24 | K-series | 2,14          | 2,24           | 1,92           | 0,12                   |
| Fe                         | 26 | K-series | 84,93         | 88,31          | 67,69              | 2,58                   | Mn                         | 25 | K-series | 2,34          | 2,44           | 1,98           | 0,14                   |
| Total: 96,17 100,00 100,00 |    |          |               |                |                    |                        | Total: 95,63 100,00 100,00 |    |          |               |                |                |                        |

a

b

**Fig. 9** Results of EDX analyses of base metal (a) and electrode remelted metal (b)

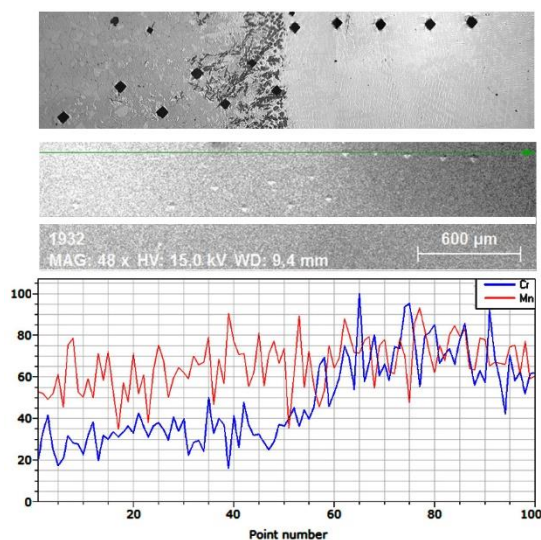


**Fig. 10** Result of EDX analyses of Cr and Mn perpendicular to fusion line

The results obtained allow concluding that rapid cooling is promising way to preserve initial wear resistant structure of retained austenite in HAZ of high-carbon low-alloyed steels during arc welding. Further investigations may be conducted to develop suitable techniques for providing rapid cooling in course of welding different machine parts produced from such steels.

#### 4 Conclusions

Investigation of structure and chemical composition of fusion layer and heat affected zone of high-carbon low-alloyed wear resistant steel quenched to retained austenite after welding leads to following conclusions.

1. Rapid cooling of welding joint is useful to obtain in HAZ fully austenitic structure that is identical to initial structure of as-quenched steel. Rapid cooling is also needed to avoid or minimize precipitation of carbides from austenite thus preventing appearance of martensite in HAZ.
2. Chemical composition of electrode metal should be adjusted in order to eliminate hardness gradient in structure of fusion line.

## References

- [1] Sarveshwar M. Reddy, Nikhil Sharma, Neeraj Gupta, Avinash Kumar Agarwal: *Fuel*, Vol. 222, 2018, p. 841-851, <https://doi.org/10.1016/j.fuel.2018.02.132>
- [2] M. Džupon, L. Kaščák, E. Spišák, R. Kubík, J. Majerníková: *Metals*, Vol. 7, 2017, No. 11, p. 515, <https://doi.org/10.3390/met7110515>
- [3] L. Kaščák, J. Mucha, E. Spišák, R. Kubík: *Strength of Materials*, Vol. 49, 2017, No. 5, p. 726-737, <https://doi.org/10.1007/s11223-017-9918-9>
- [4] R. Kubík, L. Kaščák, E. Spišák: *Koroze a Ochrana Materialu*, Vol. 60, 2016, No. 5, p. 154-161, <https://doi.org/10.1515/kom-2016-0025>
- [5] E.V. Sukhovaya: *Journal of Superhard Materials*, Vol. 35, 2013, No. 5, p. 277-283, <https://doi.org/10.3103/S106345761305002X>
- [6] R. Lencina, C. Caletti, K. Brunelli, R. Micone: *Procedia Materials Science*, Vol. 9, 2015, p. 358-366, <https://doi.org/10.1016/j.mspro.2015.05.005>
- [7] J. Viňáš, L. Kaščák: *Bulletin of Materials Science*, Vol. 31, 2008, No. 2, p. 125-131, <https://doi.org/10.1007/s12034-008-0022-4>
- [8] J. Brezinová, D. Draganovská, A. Guzanová, P. Balog, J. Viňáš: *Metals*, Vol. 6, 2016, No. 2, p. 36, <https://doi.org/10.3390/met6020036>
- [9] J. Viňáš et al.: *Materials Science Forum*, Vol. 862, 2016, p. 41-48
- [10] M. Orečný, M. Buršák, J. Viňáš: *Metalurgija*, Vol. 54, 2015, No. 1, p. 191-193
- [11] L. S. Malinov, V. L. Malinov, D. V. Burova, V. V. Anichenkov: *Journal of Friction and Wear*, Vol. 36, 2015, No. 3, p.237-240, <https://doi.org/10.3103/S1068366615030083>
- [12] V.G. Efremenko et al.: *Journal of Friction and Wear*, Vol. 34, 2013, No. 6, p. 466-474, <https://doi.org/10.3103/S1068366613060068>
- [13] A.V. Makarov, L.G. Korshunov, I.Yu. Malygina, I.L. Solodova.: *Metal Science and Heat Treatment*, Vol. 49, 2007, No. 3-4, p.150-156, <https://doi.org/10.1007/s11041-007-0028-3>
- [14] M. Šebek, F. Kováč, I. Petryshynets, J. Balko: *Materials Science Forum*, Vol. 891, 2017, p. 171-175, <https://doi.org/10.4028/www.scientific.net/MSF.891.171>
- [15] M. Šebek, L. Falat, F. Kováč, I. Petryshynets, P. Horňák, V. Girman: *Archives of Metallurgy and Materials*, Vol. 62, 2017, No. 3, p. 1721-1726, <https://doi.org/10.1515/amm-2017-0262>
- [16] M. Šebek, L. Falat, M. Orečný, I. Petryshynets, F. Kováč, M. Černík: *International Journal of Materials Research*, Vol. 109, 2018, No. 5, p. 460-468, <https://doi.org/10.3139/146.111624>
- [17] O. Hesse, J. Merker, M. Brykov, V. Efremenko: *Tribologie und Schmierungstechnik*, Vol. 60, 2013, No. 6, p. 37-43
- [18] O. Hesse, J. Liefeth, M. Kunert, A. Kapustyan, M. Brykov, V. Efremenko: *Tribologie und Schmierungstechnik*, Vol. 63, 2016, No. 2, p. 5-13
- [19] V.G. Efremenko et al.: *Wear*, Vol. 418-419, 2019, p. 24-35, <https://doi.org/10.1016/j.wear.2018.11.003>
- [20] Hong Liang Li, Duo Liu, YanYu Song, YaoTian Yan, Ning Guo, JiCai Feng: *Journal of Materials Processing Technology*, Vol. 249, 2017, p. 149-157, <https://doi.org/10.1016/j.jmatprotec.2017.06.009>

- [21] Şükrü Talaş: *Materials & Design* (1980-2015), Vol. 31, 2010, No. 5, p. 2649-2653, <https://doi.org/10.1016/j.matdes.2009.11.066>
- [22] H. Bhadeshia, R. Honeycombe: *Steels: Microstructure and Properties*, fourth ed., Elsevier, 2017
- [23] A. Devaraju, V. Kishan: *Materials Today: Proceedings*, Vol. 5, 2018, No. 1, Part 1, p. 1585-1590, <https://doi.org/10.1016/j.matpr.2017.11.250>
- [24] A. Devaraju: *Materials Today: Proceedings*, Vol. 4, 2017, No. 2, Part A, p. 3722-3727, <https://doi.org/10.1016/j.matpr.2017.02.267>
- [25] X.C. Liu, Y.F. Sun, T. Nagira, H. Fujii: *Materials Characterization*, Vol. 137, 2018, p. 24-38, <https://doi.org/10.1016/j.matchar.2018.01.004>
- [26] H. Zhang et al.: *Journal of Materials Science & Technology*, Vol. 34, 2018, No. 11, p. 2183-2188, <https://doi.org/10.1016/j.jmst.2018.03.014>
- [27] E. Curiel-Reyna, A. Herrera, V. M. Castaño, M. E. Rodriguez: *Materials and Manufacturing Processes*, Vol. 20, 2005, No. 5, p. 813-822, <https://doi.org/10.1081/AMP-200055142>
- [28] I.A. Bataev et al.: *Acta Materialia*, Volume 135, 2017, p. 277-289, <https://doi.org/10.1016/j.actamat.2017.06.038>
- [29] A. Ascari, A. Fortunato: *Optics & Laser Technology*, Vol. 56, 2014, p. 25-34, <https://doi.org/10.1016/j.optlastec.2013.07.016>
- [30] Hideki Hamatani, Yasunobu Miyazaki, Tadayuki Otani, Shigeru Ohkita: *Materials Science and Engineering: A*, Vol. 426, 2006, No. 1-2, p. 21-30, <https://doi.org/10.1016/j.msea.2006.03.024>

### **Acknowledgements**

*This work is supported by Slovak Academic Information Agency (SAIA).*